Supporting Information for *Acta Phys. -Chim. Sin.* doi: 10.3866/PKU.WHXB202007079

双功能型嵌入镍纳米颗粒的碳棱柱状微米棒电极用于电化学甲醇氧化助力的节能产氢

吕琳，张立阳，何雪冰，原弘，欧阳述昕*，张铁锐

华中师范大学，化学学院，农药与化学生物学教育部重点实验室，武汉 430079

Energy-Efficient Hydrogen Production via Electrochemical Methanol Oxidation Using a Bifunctional Nickel Nanoparticle-Embedded Carbon Prism-Like Microrod Electrode

Lin Lv, Liyang Zhang, Xuebing He, Hong Yuan, Shuxin Ouyang *, Tierui Zhang

Key Laboratory of Pesticide and Chemical Biology, Ministry of Education, College of Chemistry, Central China Normal University, Wuhan 430079, China.

*Corresponding author. Email: oysx@mail.ccnu.edu.cn

Faradaic efficiency test:

Prior to test, Ar gas was poured into the anodic electrolytes for half an hour to remove the air in the compartment and maintained at a flow rate of 20 mL·min^{-1} during the whole test. Gas chromatograph (GC) and nuclear magnetic resonance (NMR) were employed to detect the gas product and liquid product toward MOR, respectively. The faradaic efficiency toward CO_2 and formate were calculated according to the following equations:

$$FE\% = \frac{ZnF}{Q} \times 100\% \quad (1)$$

$$Q = j \times t \quad (2)$$

In equation (1), Z is the electron transfer number, n is the molar amount of substance, F is the Faraday's constant, and Q is the charge number. For equation (2), j is the measured current, t is the time.

The liquid sample was prepared as follows: 400 μL electrolyte was mixed with 100 μL D_2O and 50 μL dimethyl sulfoxide (DMSO) solution. DMSO serves as an internal standard. ^1H spectrum was obtained with water suppression using a pre-saturation method. Six electrons transfer when producing each CO_2 molecular, while four electrons transfer when generating each HCOOH molecular.

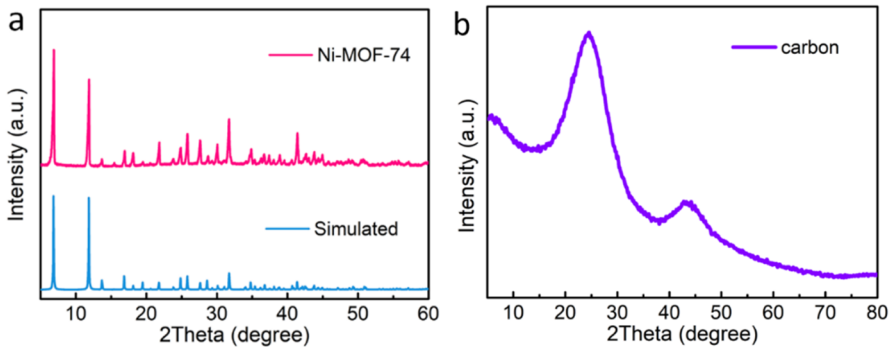

Fig. S1 XRD pattern of (a) the prepared Ni-MOF-74 and the corresponding simulated Ni-MOF-74 and (b) carbon microrods.

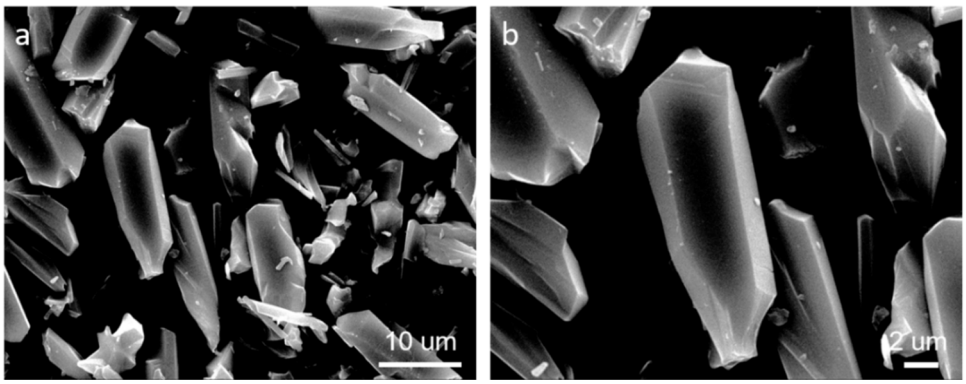

Fig. S2 FESEM images of the precursor Ni-MOF-74 with different magnifications.

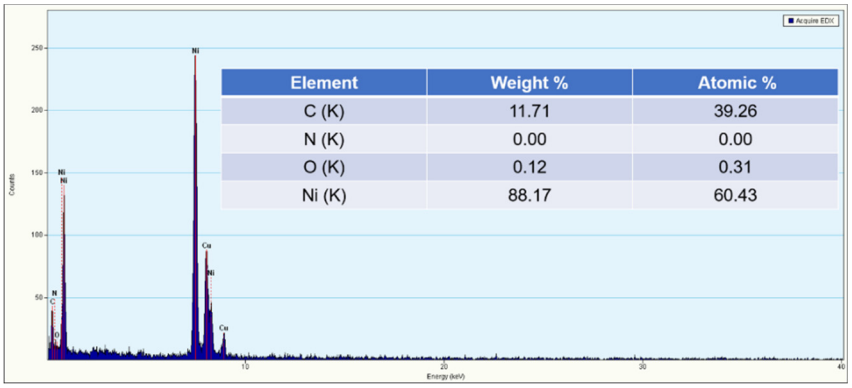

Fig. S3 TEM-EDS spectrum of the Ni@C microrods. The inset is the corresponding elemental composition.

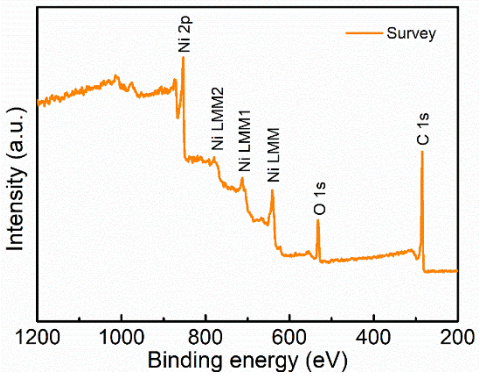

Fig. S4 XPS survey spectrum of the Ni@C microrods.

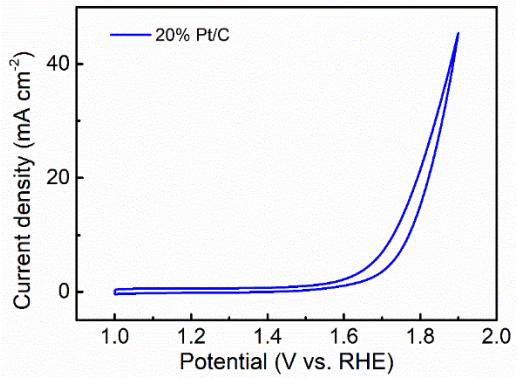

Fig. S5 CV curves of the commercial 20% (*w*) Pt/C.

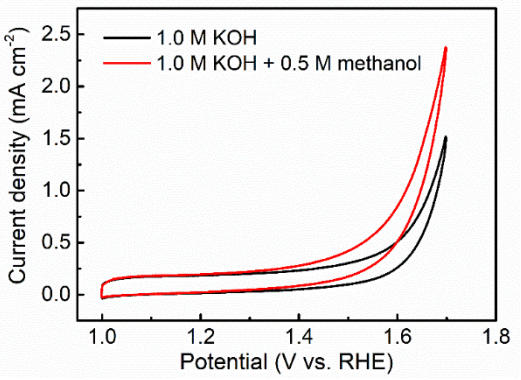

Fig. S6 The CV curves comparison of the individual C with the presence and absence of methanol at the scan rate of 50 mV·s^{-1}.

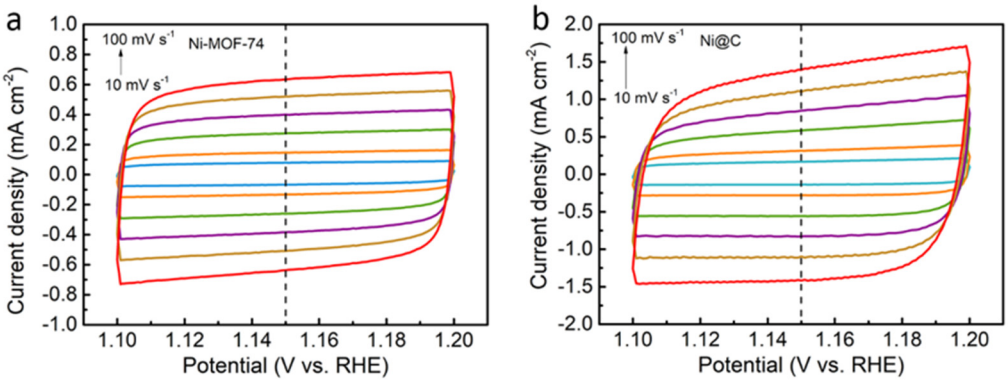

Fig. S7 CV curves of (a) the Ni-MOF-74, (b) the Ni@C at a potential range of 1.10–1.20 V.

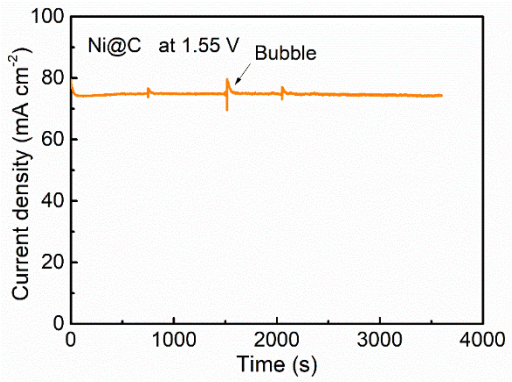

Fig. S8 Chronopotentiometry test of the Ni@C at a potential of 1.55 V (*vs* RHE).

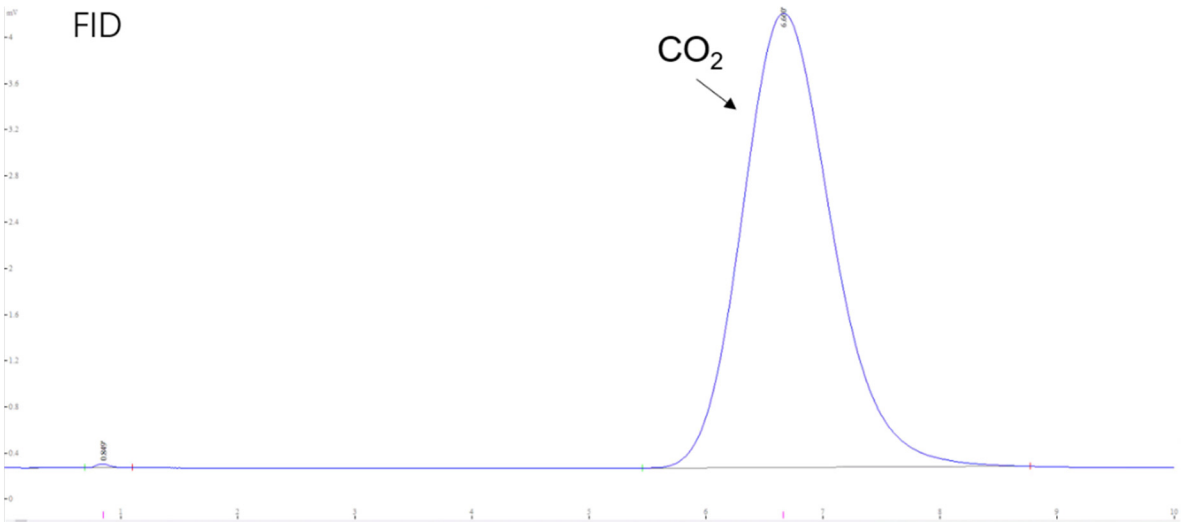

Fig. S9 Gas chromatogram of the gas product during the online test at the potential of 1.55 V (*vs* RHE).

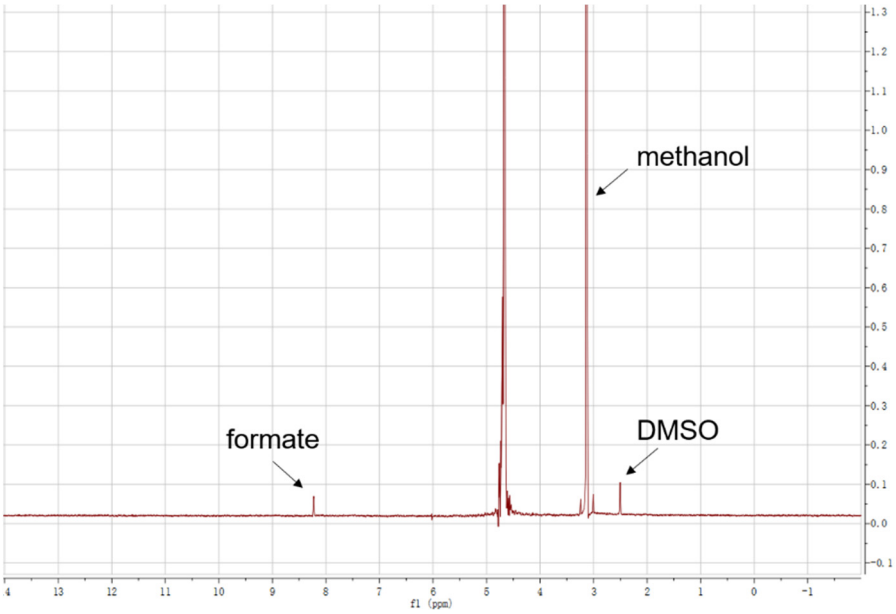

Fig. S10 ^{1}H-NMR spectra of the liquid sample obtained at the potential of 1.55 V (*vs* RHE).

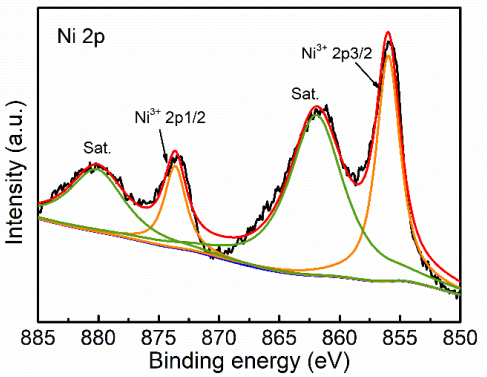

Fig. S11 High-resolution XPS spectrum for Ni 2*p* of the Ni@C after 12-h MOR test.

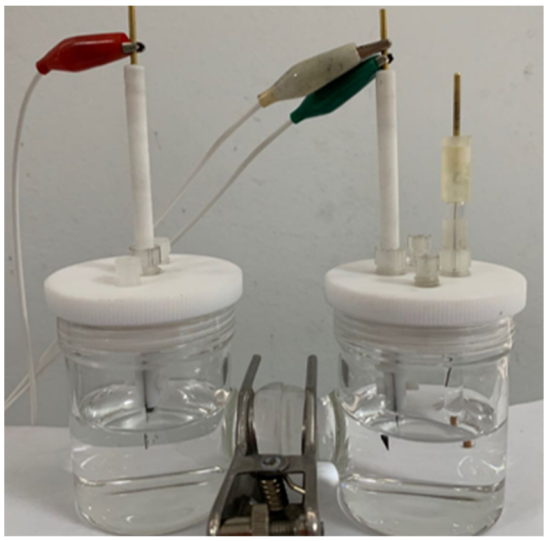

Fig. S12 Photograph of the electrochemical hybrid test system.

Table S1 Elemental composition of surface/subsurface of the Ni@C from the XPS data.

Sample	Content (atomic fraction, %)		
	Ni	C	O
Ni@C	9.83	75.76	14.41

Table S2 Methanol electro-oxidation performance of some recently reported Ni-based electrocatalysts.

Catalysts	Mass-normalized current density ($mA \cdot mg^{-1}$)	Potential (V *vs* RHE)	Methanol concentration	Electrolyte	Substrate	Year published	Ref.
$[(Ni, Co)(OH)_4]$ clusters in MOFs	527	1.465	1 $mol \cdot L^{-1}$	0.1 $mol \cdot L^{-1}$ KOH	Glassy carbon	2019	1
Ni/NiO heterostructures	2094	1.504	1 $mol \cdot L^{-1}$	1 $mol \cdot L^{-1}$ KOH	Glassy carbon	2017	2
NiCu alloy	1028	1.55	1 $mol \cdot L^{-1}$	1 $mol \cdot L^{-1}$ KOH	Glassy carbon	2020	3
Ni/rGO	1600	1.623	1 $mol \cdot L^{-1}$	1 $mol \cdot L^{-1}$ KOH	Glassy carbon	2018	4
Ni-NiO@C	210	1.766	0.5 $mol \cdot L^{-1}$	1 $mol \cdot L^{-1}$ KOH	Glassy carbon	2018	5
Ni@C microrods	111.8	1.500	0.5 $mol \cdot L^{-1}$	1 $mol \cdot L^{-1}$ KOH	Carbon paper	–	This work

References

(1) Wu, Y. P.; Tian, J. W.; Liu, S.; Li, B.; Zhao, J.; Ma, L. F.; Li, D. S.; Lan, Y. Q.; Bu. X. *Angew. Che*m. *Int. Ed.* **2019,** *58*, 12185. doi: 10.1002/anie.201907136

(2) Wang, J.; Teschner, D.; Yao, Y.; Huang, X.; Willinger, M.; Shao, L.; Schlögl, R. *J. Mater. Chem. A* **2017,** *5*, 9946. doi: 10.1039/C7TA01982C

(3) An, Y.; Ijaz, H.; Huang, M.; Qu, J.; Hu. S. *Dalton Trans.* **2020,** *49*, 1646. doi: 10.1039/C9DT04661E

(4) Sun, H.; Ye, Y.; Liu, J.; Tian, Z.; Cai, Y.; Li, P.; Liang, C. *Chem. Commun.* **2018,** *54*, 1563. doi: 10.1039/C7CC09361F

(5) Yu, J.; Ni, Y.; Zhai. M. *J. Phys. Chem. Solids* **2018,** *112*, 119. doi: 10.1016/j.jpcs.2017.09.022